



Modeling and prediction of optimal process parameters in wear behaviour of selective inhibition sintered high density polyethylene parts

Balasubramanian Esakki¹ · D. Rajamani¹ · P. Arunkumar¹

Received: 16 June 2017 / Accepted: 21 November 2017 / Published online: 28 November 2017
© Springer International Publishing AG, part of Springer Nature 2017

Abstract

Owing to the dependency of multiple process parameters in additive manufacturing (AM) techniques, it is tedious to determine optimal processing conditions for improving quality characteristics of fabricated functional parts. The present study focuses on optimization of four key contributing parameters such as layer thickness, heater energy, heater feedrate, and printer feedrate on dry sliding wear behaviour of high-density polyethylene (HDPE) parts fabricated through a novel selective inhibition sintering (SIS) process. The experiments are conducted on the basis of response surface methodology (RSM) and four factor-three level box-behnken design. The significance of the developed models and contribution of each process parameters on wear rate are estimated through analysis of variance (ANOVA). The results suggested that wear rate is influenced principally by the layer thickness and heater energy. The quadratic regression model of RSM associated with the desirability approach is employed to determine optimum levels of process parameters. The morphologies of worn surfaces are observed using scanning electron microscope. Sensitivity analysis has been performed to measure the relative impact of SIS process parameters on wear rate.

Keywords Selective inhibition sintering · Response surface methodology · Wear rate · Optimization · ANOVA · Desirability · Sensitivity · Morphology

1 Introduction

Industries are demanding disruptive technologies to adapt changes swiftly and to remain competitive in the market. Time-to-market is the key issue in product design and development. The high strength, durable, non-corrosive and light-weight products are of prime importance in the present industrial scenario. On account of this, emergence of rapid prototyping (RP) technology to fabricate prototypes, functional parts and concept model at relatively lower cost compared with traditional subtractive and other manufacturing processes has attracted plethora of industries. RP is used to build three-dimensional (3D) objects directly from the computer-aided design (CAD) data and it has proven to

be a key enabling technology by reducing 60% of lead time compared with traditional manufacturing process during product development process [1]. RP processes are classified according to the physical characteristics of raw material used to develop the product [2]. Stereolithography [3] is a well-established liquid based system and widely used in many industries. Solid-based, importantly, fused deposition modelling technique [4] is attractive due to its versatility in producing high-strength parts. In recent times, powder-based RP techniques are playing a vital role in medium-to-high volume series production. Selective laser sintering (SLS) has become prevalent because it does not necessitate any support structure and the post processing is quite easy [5]. It employs high-power CO₂ laser to exhibit sintering of polymer powder at the desired surface area. Due to the utilization of extraordinary laser system, the cost of the machine is high. Eliminating laser technology in RP processes has tremendous impact in the reduction of cost of machine and increases speed of the process. Owing to this fact, high-speed sintering (HSS) process [6] has been developed which employs low-cost infra-red heater to sinter polymer powder particles.

✉ D. Rajamani
rajamanitamil1991@gmail.com

¹ Centre for Autonomous System Research (CASR),
Department of Mechanical Engineering, Veltech Dr.RR &
Dr.SR University, Chennai 600062, India

This process utilizes radiation absorbent material (RAM) to absorb and transfer heat to the polymers through which sintering phenomenon is achieved [7]. However, availability of RAM and more wastage of polymer powder material are main challenges to accustom HSS. The production cost of the product is influenced by machine cost and speed of the process. These two aspects are to be strengthened with a competitive RP process to produce parts of high volume.

In view of this, a novel layer-by-layer manufacturing process called selective inhibition sintering (SIS) is developed by University of Southern California, USA [8]. In this process, indigenous polymer powders and low-cost heaters can be utilized that significantly reduce the machine cost. The working mechanism of SIS is sintering of polymer powder particles in the desired surface region and inhibition at the part boundary [9]. SIS has significant advantages in terms of eliminating the expensive tooling and support structure, and it can handle wide range of polymers, ceramic and metal powders unlike FDM that makes the system cost effective. However, there are tremendous challenges to achieve superior part quality, enhanced part strength, high-dimensional accuracy, improved surface quality, and maximum wear resistance. Hence, it is essential to understand the performance of SIS process in relation to variation of input process variables so that the process can be made reliable for functional part production. In SIS, many factors influence the part quality such as layer thickness, sintering temperature, heater feedrate, part bed temperature, printer pressure, and printer feedrate [10]. Wear resistance is an important characteristic for the durability of parts and minimal extents of studies are undertaken to understand the wear mechanism of RP processed specimens.

Equbal et al. [11] have proposed that wear resistance of acrylonitrile butadiene styrene (ABS) parts produced by FDM can be improved by reducing the distortion. They have reported that wear can occur due to the formation and breaking of interfacial adhesive bonds, scratching, and fatigue. Sood et al. [12] have studied and optimized the influence of various FDM process parameters on wear rate of ABS parts using artificial neural network and particle swarm optimization technique. Kumar et al. [13] confirmed that parts produced by selective laser sintering (SLS) process can exhibit better wear performance when compared with selective laser melting (SLM) process. Ramesh et al. [14] have premeditated the sliding wear performance of iron–silicon carbide composite fabricated through SLS process. They concluded that low amount of usage of laser power exhibits higher wear resistance, higher density, and micro hardness. It is evident from literature that none of the researchers have attempted their investigation to understand the effect of process parameters on dry sliding wear behaviour of SIS processed parts. Therefore, the present study investigates on the wear characteristics of SIS fabricated HDPE parts and its influence with

various process parameters such as layer thickness, heater energy, heater feedrate, and printer feedrate. In order to perform parametric analysis and building an empirical model of the process, a box-behnken design (BBD) methodology is adopted. Interaction of process parameters is studied using response surface methodology (RSM) and further optimized through desirability approach to achieve desired wear rate. In addition, scanning electron microscope (SEM) analysis has been performed to investigate the morphologies of worn surfaces. Further, the quantitative effect of process parameters on wear rate is obtained using sensitivity analysis.

2 Experimental procedures

2.1 Experimental set-up

Experiments are conducted using a custom built SIS machine and its schematic is illustrated in Fig. 1. The machine consists of a ceramic heater with 500 W capacity, inhibitor nozzle which is connected with inhibition reservoir, a powder feeding roller, recycle tank, and an effective built chamber with a volume of $250 \times 250 \times 150 \text{ mm}^3$. A 3D CAD model of the part is sliced with minimal layer thickness and boundary of the part is defined during machine tool path generation. Based on this, heater traverses along longitudinal direction to apply heat on parts surface through which sintering phenomenon is achieved. A nozzle system delivers inhibitor solution to avoid excessive heating of polymer powders and provide region of separation for easy removal of part during post-processing. The layer-by-layer fabrication process continued until the desired 3D part is fabricated.

2.2 Materials

The high-density polyethylene (HDPE) powder supplied by J.P. Polymers, India, with an average particle size ranging about 35–80 μm is used in this process and the test specimens fabricated in this work are intended to be used in small armament applications. The microstructure of as received HDPE powder distribution is depicted in Fig. 2 and the properties are given in Table 1. It is observed that most of the polymer particles resemble ellipsoidal shape and it has high melting point which is advantageous for high-temperature applications. It has potential applications in advanced engineering materials such as ballistic plates, fuel tanks and especially small armament appliances (magazine, hand grips and casings) due to its enhanced properties such as high strength-to-weight ratio, high corrosion resistance, dimension stability and stronger intermolecular forces. In this study, Potassium Iodide (KI) extra pure crystals dissolved in distilled water and isopropyl alcohol is used as inhibitor solution to perform inhibition sintering of polymer particles.

Fig. 1 Schematic layout of SIS process

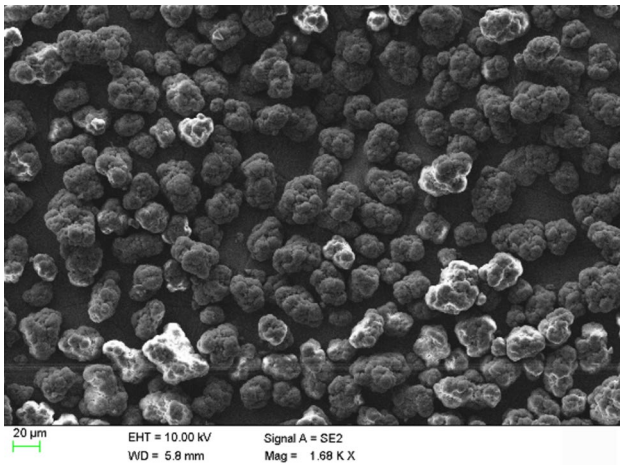
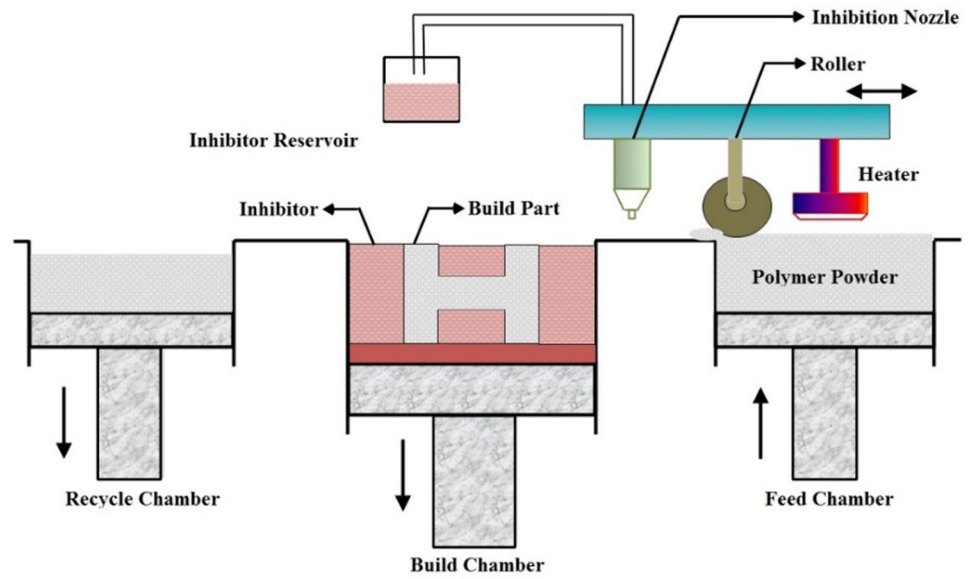


Fig. 2 Microstructure of HDPE raw powder

Table 1 Properties of HDPE

| | |
|--|-----------------------|
| Melting point (°C) | 178 |
| Density (kg/m ³) | 940 |
| Coefficient of thermal expansion (/°C) | 12 × 10 ⁻⁵ |
| Tensile strength (MPa) | 21–24 |
| Thermal conductivity (W/m K) | 0.49 |

2.3 Selection of process parameters

The SIS process includes a large number of input process parameters such as layer thickness, roller feedrate, printer feedrate, heater feedrate, sintering temperature, and built tank temperature. Among these parameters, the following

Table 2 Process parameters and their levels

| Parameter | Unit | Level | | |
|----------------------|-------------------|-------|-------|-------|
| | | - 1 | 1 | 0 |
| Layer thickness (A) | mm | 0.1 | 0.2 | 0.15 |
| Heater energy (B) | J/mm ² | 22.16 | 28.48 | 25.32 |
| Heater feedrate (C) | mm/s | 3 | 3.5 | 3.25 |
| Printer feedrate (D) | mm/min | 100 | 120 | 110 |

four important process variables are considered in this study to fabricate HDPE specimens:

Layer thickness (A) The thickness of the layer deposited by the roller and depends upon the feed of the roller.

Heater energy (B) The amount of heat energy transferred from the ceramic heater to the powder bed to sinter the polymer particles.

Heater feedrate (C) The speed of the ceramic heater at which it moves across the build chamber.

Printer feedrate (D) The speed of the inhibitor print nozzle at which it prints the inhibition pattern across the surface of part bed.

The heater energy is selected based on the type of powder to be used for fabricating the specimens. It is well known that the assortment of heat energy dominates the sintering phenomenon. An exhaustive pilot experimentation has been performed in order to reduce the fabrication errors and to decide the working range of each control parameters. The selected process parameters at three different levels with their ranges to perform experimental studies are given in Table 2. The remaining process parameters such as roller feedrate (5 mm/s), built tank temperature (50 °C), and stand-off distance (5 mm) are kept constant throughout the experiments.

2.4 Experimental design

Response surface methodology (RSM) is an empirical statistical modelling technique utilized for multiple regression analysis wherein quantitative data are obtained through designed experiments [15]. RSM can be used for optimizing complex processes with reduced number of experimental trails to evaluate multiple independent variables and their interactions. In this study, RSM is used to optimize and study the effect of independent variables such as layer thickness, heater energy, heater feedrate and printer feedrate on the wear rate. The experiments are established based on box-behnken design (BBD) with four factors at three levels between -1 , 0 and $+1$ corresponding to low, middle and high levels (Table 1). The variables are coded by the following equation:

$$x_i = \frac{X_i - X_0}{\Delta X} \quad i = 1, 2, 3, \dots, k, \quad (1)$$

where x_i and X_i are dimensionless value and real value of an independent variables, X_0 is real value of an independent variable at the centre point and ΔX is the step change value of the variable. The BBD is a spherical, revolving design; it consists of a central point and middle points of edges of the cube circumscribed on sphere [16]. It has been applied in the optimization of process parameters in which one is not interested in predicting extreme responses. The number of experiments (N) required for the development of BBD is defined as $N = 2k(k - 1) + C_0$ (where k is number of factors and C is number of central point). In general, the linear model is insufficient for a mathematical description of a research problem with an adequate precision. Hence, the mathematical model of the experimental data gives the second-order polynomial equation for the optimization of the process parameters. The following second-order polynomial model explains the behaviour of the system as follows:

$$y = \beta_0 + \sum_{i=1}^k \beta_i x_i + \sum_{i=1}^k \beta_{ii} x_i^2 + \sum_i \sum_j \beta_{ij} x_i x_j + \epsilon, \quad (2)$$

where y is the response and x_i are the values of i^{th} SIS process parameter; β_0 is model constant; β_i represents linear coefficient; β_{ii} denotes quadratic coefficient; β_{ij} is the interaction coefficient; k corresponds to number of variables; and ϵ indicates statistical experimental error.

2.5 Specimen preparation

The wear specimen of length 50 mm and diameter of 6 mm is modelled and exported as a stereolithographic (.stl¹) file. Further, .STL (surface tessellation language) file is sliced into layers using *slice3r* software with required layer thickness to get contour information of each layer and converted into G-codes. Finally, G-code data are sent to the SIS system (*Pronterface*) for specimen fabrication. All test specimens are fabricated using virgin HDPE powders and process parameters are set as per experimental plan (Table 3). During the course of experiments, initially polymer powder (HDPE) are filled in the feed chamber and inhibitor tank is filled with potassium iodide (KI) solution. Then the powder is fed by a roller with specified layer thickness, at the same time selected part area is inhibited through inhibitor nozzle to prevent powder from sintering. Here, surplus powder is warehoused into a separate recycle chamber which is bounded parallel to part fabrication chamber. A ceramic heater is moved above and along the build chamber to achieve sintering of polymer powder. The sequence of deposition, inhibition and sintering is continued until realization of desired 3D specimen. Finally, the part is removed from built chamber and post processing including cleaning of inhibitor from the part and removing excess unsintered powder from part surface completes the SIS process.

2.6 Wear testing

Dry sliding wear tests are conducted on a pin-on-disc wear testing apparatus (Ducom-TR-20LE) as shown in Fig. 3. The cylindrical pin specimens of 6 mm diameter and 50 mm length are tested against EN 45 steel disc of 65 HRC. The test specimen having flat end contact surface is positioned perpendicular to flat circular disc. The contact path diameter is set as 120 mm and disc is made to rotate with constant speed of 1 m/s. A constant weight of 25 N is applied parallel to the axis of specimen. Wear volumes (mm^3/m) are measured by multiplying cross sectional area with decrease in height and also sliding distance (m) is obtained by multiplying time with speed of rotation [12]. The initial wear volume is not uniform because of higher surface roughness and presence of foreign materials in the specimen. Hence, true wear rate is calculated after removing foreign materials through break in period. As initial wear data possess non-linear relationship between wear volumes and sliding distance, it is regarded as transient wear region data and neglected. Beyond transient region, complete contact between the disc

¹ “stl” is used by the company 3D Systems as an data file format for their stereo lithography machine; stl was never standardized.

Table 3 Experimental design matrix and collected data

| Std. No. | Run | Parameters | | | | Response |
|----------|-----|----------------------|------------------------------------|------------------------|---------------------------|--------------------------------|
| | | Layer thickness (mm) | Heater energy (J/mm ²) | Heater feedrate (mm/s) | Printer feedrate (mm/min) | Wear rate (mm ³ /m) |
| 1 | 26 | 0.10 | 22.16 | 3.25 | 110 | 0.0425 |
| 2 | 16 | 0.20 | 22.16 | 3.25 | 110 | 0.0376 |
| 3 | 25 | 0.10 | 28.48 | 3.25 | 110 | 0.0217 |
| 4 | 27 | 0.20 | 28.48 | 3.25 | 110 | 0.0416 |
| 5 | 22 | 0.15 | 25.32 | 3.00 | 100 | 0.0377 |
| 6 | 19 | 0.15 | 25.32 | 3.50 | 100 | 0.0289 |
| 7 | 8 | 0.15 | 25.32 | 3.00 | 120 | 0.0238 |
| 8 | 7 | 0.15 | 25.32 | 3.50 | 120 | 0.0395 |
| 9 | 24 | 0.10 | 25.32 | 3.25 | 100 | 0.0255 |
| 10 | 5 | 0.20 | 25.32 | 3.25 | 100 | 0.0468 |
| 11 | 6 | 0.10 | 25.32 | 3.25 | 120 | 0.0333 |
| 12 | 29 | 0.20 | 25.32 | 3.25 | 120 | 0.033 |
| 13 | 28 | 0.15 | 22.16 | 3.00 | 110 | 0.0401 |
| 14 | 2 | 0.15 | 28.48 | 3.00 | 110 | 0.0291 |
| 15 | 15 | 0.15 | 22.16 | 3.50 | 110 | 0.0373 |
| 16 | 9 | 0.15 | 28.48 | 3.50 | 110 | 0.0323 |
| 17 | 18 | 0.10 | 25.32 | 3.00 | 110 | 0.0341 |
| 18 | 13 | 0.20 | 25.32 | 3.00 | 110 | 0.0416 |
| 19 | 3 | 0.10 | 25.32 | 3.50 | 110 | 0.0335 |
| 20 | 1 | 0.20 | 25.32 | 3.50 | 110 | 0.0451 |
| 21 | 12 | 0.15 | 22.16 | 3.25 | 100 | 0.0411 |
| 22 | 11 | 0.15 | 28.48 | 3.25 | 100 | 0.0264 |
| 23 | 14 | 0.15 | 22.16 | 3.25 | 120 | 0.0309 |
| 24 | 23 | 0.15 | 28.48 | 3.25 | 120 | 0.0307 |
| 25 | 21 | 0.15 | 25.32 | 3.25 | 110 | 0.0349 |
| 26 | 17 | 0.15 | 25.32 | 3.25 | 110 | 0.0368 |
| 27 | 10 | 0.15 | 25.32 | 3.25 | 110 | 0.0353 |
| 28 | 20 | 0.15 | 25.32 | 3.25 | 110 | 0.0344 |
| 29 | 4 | 0.15 | 25.32 | 3.25 | 110 | 0.0373 |

**Fig. 3** Pin-on-disc wear test experimental setup

and specimen is ensured and wear is considered as the true wear rate of the specimen under operating conditions.

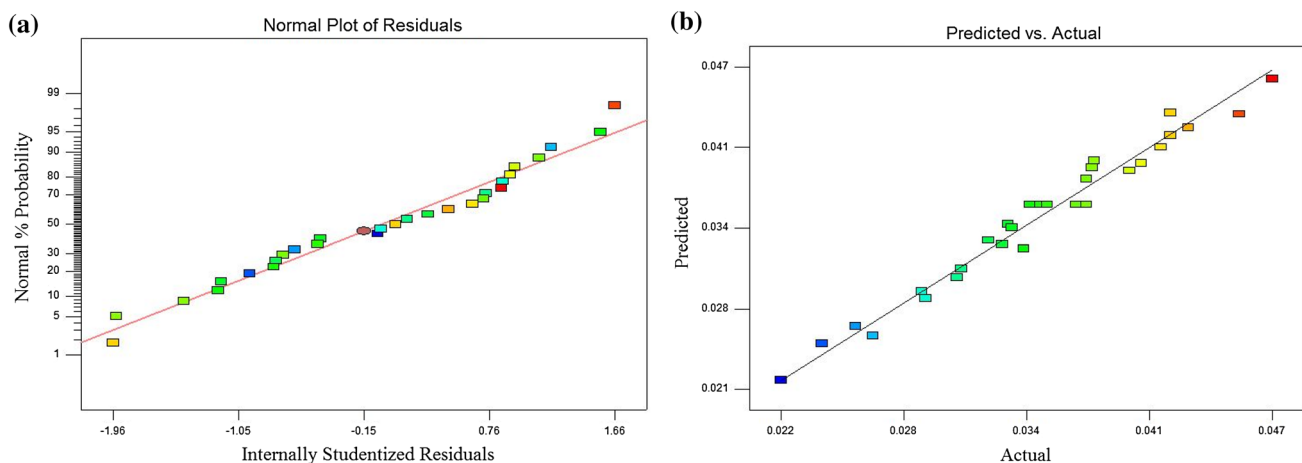
3 Results and discussion

3.1 Statistical analysis and development of empirical model

The statistical analysis is performed using Design expert statistical software 7.0.0 (Stat Ease Inc.). The experimental data are analysed using analysis of variance (ANOVA) and significance of developed models is evaluated through F test. The ANOVA results shown in Table 4 describe that F value of 48.631 indicates that model is adequate for prediction of wear rate. Moreover, the model “Prob > F ” value of less than 0.05 (i.e., $\alpha = 0.05$ or 95% confidence level) shows that this model is significant, which is desirable as it demonstrates

Table 4 Analysis of variance (ANOVA) results

| Source | Sum of squares | DOF | Mean square | F value | Prob > F | Remarks |
|--------------------|----------------|---------------|-------------|---------|--------------------|-----------------|
| Model | 0.00105 | 12 | 8.81E-05 | 48.631 | 0.0001 | Significant |
| A-layer thickness | 0.00025 | 1 | 0.00025 | 139.505 | 0.0001 | |
| B-heater energy | 0.00018 | 1 | 0.00018 | 104.55 | 0.0001 | |
| C-heater feedrate | 8.67E-06 | 1 | 8.67E-06 | 4.780 | 0.0440 | |
| D-printer feedrate | 1.92E-05 | 1 | 1.92E-05 | 10.616 | 0.0049 | |
| AB | 0.00015 | 1 | 0.00015 | 84.784 | 0.0001 | |
| AD | 0.00011 | 1 | 0.00011 | 64.315 | 0.0001 | |
| BC | 9E-06 | 1 | 9E-06 | 4.962 | 0.0406 | |
| BD | 5.25E-05 | 1 | 5.25E-05 | 28.983 | 0.0001 | |
| CD | 0.00015 | 1 | 0.00015 | 82.745 | 0.0001 | |
| A ² | 2.34E-05 | 1 | 2.34E-05 | 12.914 | 0.0024 | |
| B ² | 1.06E-05 | 1 | 1.06E-05 | 5.880 | 0.0275 | |
| D ² | 5.94E-05 | 1 | 5.94E-05 | 32.756 | 0.0001 | |
| Residual | 2.9E-05 | 16 | 1.81E-06 | | | |
| Lack of fit | 2.27E-05 | 12 | 1.89E-06 | 1.213 | 0.4654 | Not significant |
| Pure error | 0.000006 | 4 | 0.000001 | | | |
| Cor. total | 0.00108 | 28 | | | | |
| | | $R^2=97.33\%$ | | | $Adj. R^2=95.33\%$ | |

**Fig. 4** Normal probability and predicted vs actual plots for experimental runs

that terms in the model have a significance on wear rate. This table also shows that layer thickness and heater energy have significant effect on wear rate, whereas printer feedrate and heater feedrate are not much influenced. The coefficient of determination (R^2) for wear rate is found to be 97.33%, which approaches to unity. This confirms that developed model can better fit to actual data. The adjusted coefficient of determination ($Adj. R^2$) value of 95.33% enables that developed model from experimental data is reasonably accurate and the relationship generated is satisfactory.

The diagnostic plots such as normal probability plot of residuals and predicted versus actual plots (Fig. 4a, b) are

used to evaluate the model satisfactoriness and also exhibiting relationship between experimental and predicted values. From these figures, each of the observed values is compared to predicted value from the model. It also illustrates that residuals are normally distributed and lie reasonable close to the straight line. Hence, it can be concluded that the proposed models are adequate and there is no reason to suspect any violation of independence or constant variance assumption [17].

The empirical relationship between experimental results of BBD model and regression coefficients of second-order polynomial equation is obtained by removing

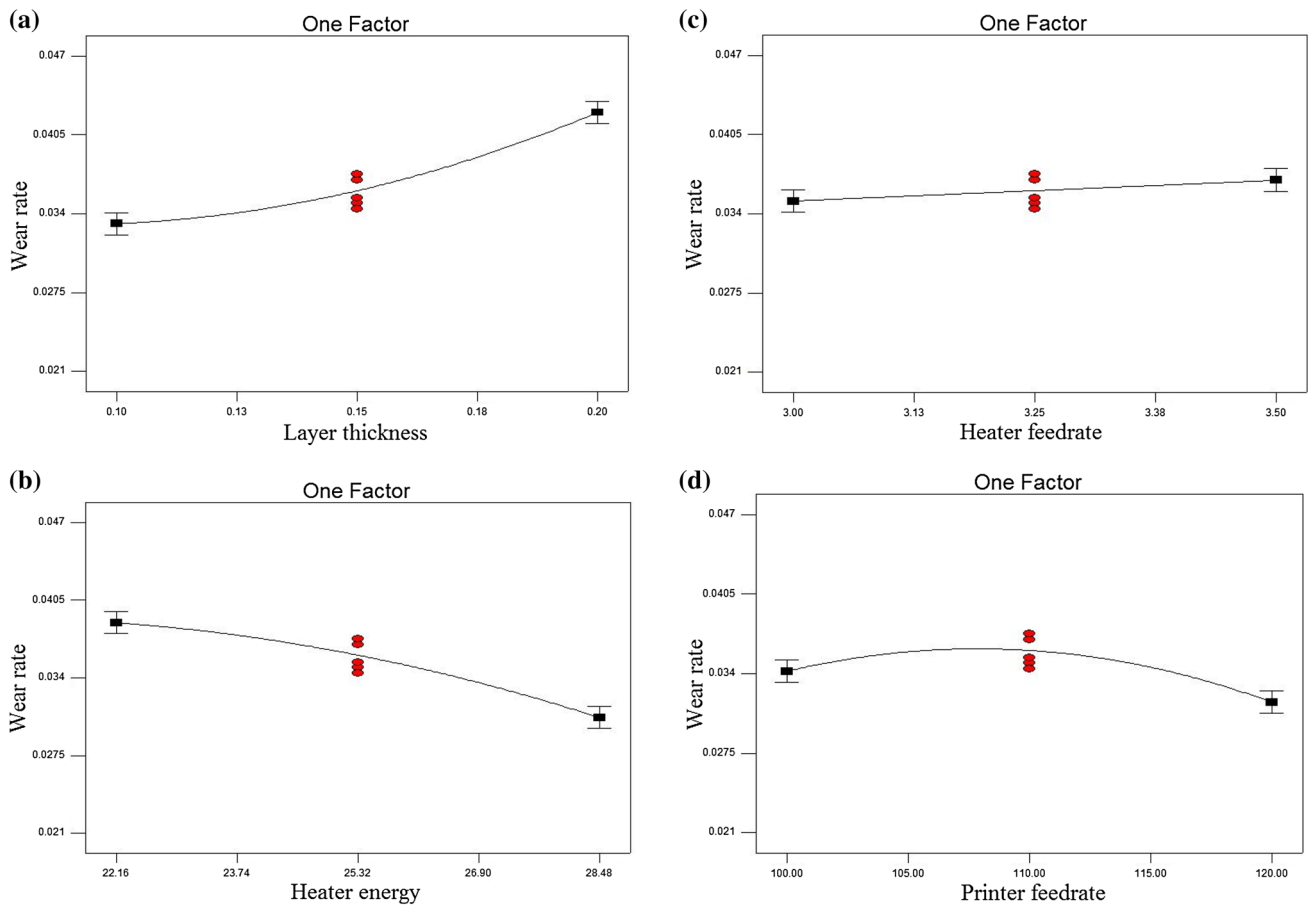


Fig. 5 Effect of process parameters on wear rate

insignificant terms in the developed model. The final regression relation to estimate wear rate as a function of four input process parameters is given by:

$$\begin{aligned}
 \text{Wear rate (mm}^3/\text{m)} = & 0.9557 + 0.0623 \times A - 0.0195 \times B \\
 & - 0.3141 \times C - 0.0028 \times D \\
 & + 0.0392 \times A \times B - 0.0108 \times A \times D \\
 & + 0.0018 \times B \times C + 0.0001 \times B \times D \\
 & + 0.0024 \times C \times D + 0.7463 \times A^2 \\
 & - 0.0001 \times B^2 - 3 \times 10^{-5} \times D^2.
 \end{aligned}
 \tag{3}$$

The quadratic regression model represents response for wear rate parameter, where *A* is layer thickness, *B* is heater energy, *C* is heater feedrate and *D* is printer feedrate, *AB* is interaction factor between layer thickness and heater energy, *AD* is interaction factor between layer thickness and printer feedrate, *BC* is interaction factor between heater energy and heater feedrate, *BD* is interaction factor between heater energy and printer feedrate, *CD* is the interaction factor between heater feedrate and

printer feedrate and *A*², *B*², *D*² are the quadratic effect of layer thickness, heater energy and printer feedrate, respectively.

3.2 Relationship between wear rate and process parameters

Based on the developed response surface models, it is found that all the four selected parameters such as layer thickness, heater energy, heater feedrate and printer feedrate have a significant effect on wear rate. Hence, it is necessary to establish the relationship between the wear rate and the process variables. The individual effects of selected process variables on wear rate are depicted in Fig. 5a–d.

3.2.1 Effect of layer thickness

The increase of layer thickness from 0.1 to 0.2 mm tends to increase the wear rate as observed in Fig. 5a. When the layer thickness is low, sufficient heat energy infiltrates into thin powder layer which causes strong

bonding between powder particles thereby dense parts are obtained. Due to strong intermolecular attraction of polymer particles, the mechanical properties are enhanced which lead to minimized wear rate. As the layer thickness increases from its low level to high level, the uniform thermal stress is not developed at deposited materials due to non-uniform temperature gradients resulting thermal distortion in sintered layers. Therefore, the wear rate increases with increase in layer thickness because of the domination effect of distortion in bonding.

3.2.2 Effect of heater energy

Heater energy has a significant effect on wear rate, as revealed in Fig. 5b. It can be seen that there is a reduction in wear rate as the heater energy increases from 22.16 to 28.48 J/mm². As the heat energy increases from its low level to high level, the inter-particle bonding between the powder particles become stronger due to better fusion, resulting in increase in part strength and wear resistance.

3.2.3 Effect of heater feedrate

Wear rate has increased with respect to increase in heater feedrate from low level (3 mm/s) to high level (3.5 mm/s) as depicted in Fig. 5c. This can be attributed due to the fact, at higher heater feedrate, energy absorbed by polymer powder for a fixed time interval per unit area has shorter heating time resulting in improper sintering and weak bonding of powder particles causes poor wear strength. On the contrary, lower heater feedrate increases the contact time between the heater and powder bed. Hence, sufficient heat energy is spread over the powder surface and temperature fields tend to be uniform, ensuing in the formation of compact structure with higher wear resisting characteristics.

3.2.4 Effect of printer feedrate

It can be seen from Fig. 5d, increase of printer feedrate from 100 to 120 mm/min slightly reduces wear rate. Also printer feedrate is not much influencing on wear rate, because the inhibitor solution is inhibited at the periphery of the part profile that affects only at the boundary of specimen. However, at a low printer feedrate, inhibition spell is increased and it penetrates apart from the actual targeted regions. This leads to prevent powder from effective sintering. Hence, wear resistance is decreased due to inappropriate sintering of polymer powders. Moreover, the inhibition printing time depends on geometrical complexity and thickness of each layer.

3.3 3D response surface plots for wear rate

The response surface plots shown in Fig. 6a–c depicts the interaction effect of various process parameters on wear rate. The consequence of layer thickness and heater energy on wear rate shown in Fig. 6a describes that at higher heater energy minimal wear rate is obtained. However, wear rate is increased with increase of layer thickness. The minimum wear rate of 0.0229 mm³/m is achieved at high heater energy of 28.48 J/mm² and low layer thickness of 0.1 mm. Increasing layer thickness and printer feedrate have increased wear rate as observed in Fig. 6b. Least wear rate of 0.0212 mm³/m is obtained at lower layer thickness of 0.1 mm with minimal printer feedrate of 100 mm/min. Decrease in wear rate is attained for higher heater energy and influence of heater feedrate has not affected wear rate as seen from Fig. 6c. The minimum wear rate of 0.0295 mm³/m is found at a combination of high heater energy (28.48 J/mm²) and low heater feedrate of 3 mm/s.

3.4 Optimization using desirability approach

Prediction of optimal process parameters in minimizing wear rate is a challenging task in SIS process due to the presence of a large number independent variables and complicated stochastic process mechanism. In view of this, RSM based desirability optimization approach [18] is used in which the wear rate is ‘minimized’ and for the factors are ‘within range’. In addition, weights are assigned for each response ranging from 0.1 to 10 to adjust the shape of its particular desirability function. The importance of process variables is varied from the least to most desirable (i.e., 1 and 5). From the desirability-based approach, varied best solutions are obtained and the solution with highest desirability is preferred. The best optimized conditions are obtained at desirability of 1.00 for minimal wear rate of 0.0209 mm³/m: layer thickness 0.11 mm, heater energy 27.88 J/mm², heater feedrate 3.00 mm/s, and printer feedrate 118.78 mm/min which is shown in desirability ramp function (Fig. 7) In the desirability ramp function, the dot of each ramp denotes reflection of parameter setting and height of the dot indicates the amount of desirability [19]. Further, contour plots for overall desirability are depicted in Fig. 8 to comprehend the sensitivity of optimization results. From the contour plot, the optimal region is located at the left corner part of graph that indicates the desirability value of 1.00, which contests the target value.

In order to predict and verify identified optimal process parameters on determining wear rate, confirmation experiments are performed. Each of the confirmation experiments is repeated three times and the average values have been considered. Table 5 shows the predicted and actual values of wear rate and its percentage of error

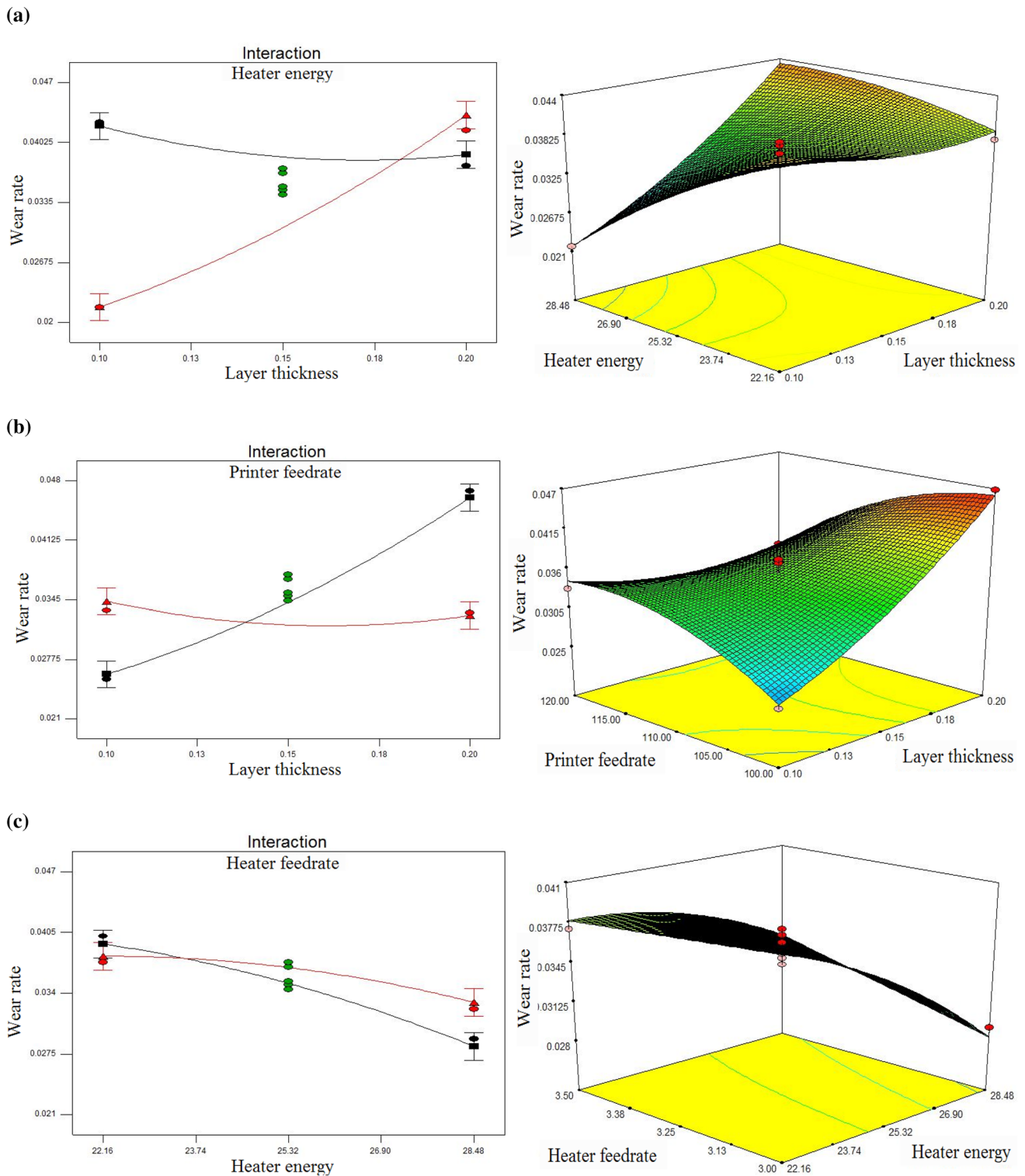


Fig. 6 Interaction and 3D response surface plots for wear rate. **a** Layer thickness and heater energy, **b** layer thickness and printer feedrate, and **c** heater energy and heater feedrate

during experimental validation of the developed model. The results suggested that the difference between predicted and actual value is below 5% which signifies that

the developed model is suitable for predicting the wear rate of SIS processed parts.

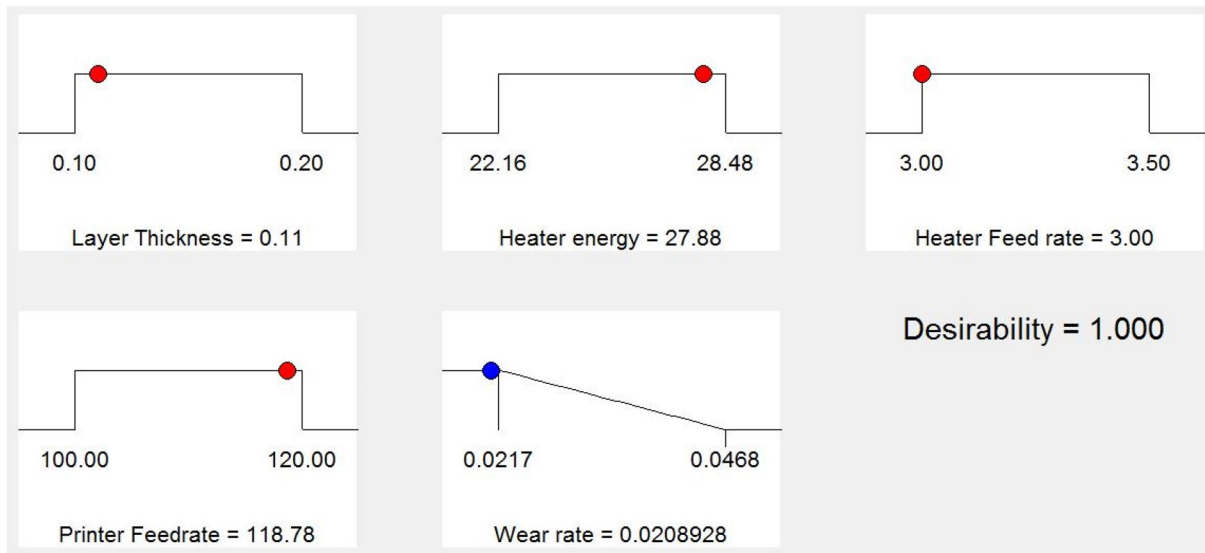


Fig. 7 Desirability ramp function of numerical optimization

Fig. 8 Contour plot for desirability

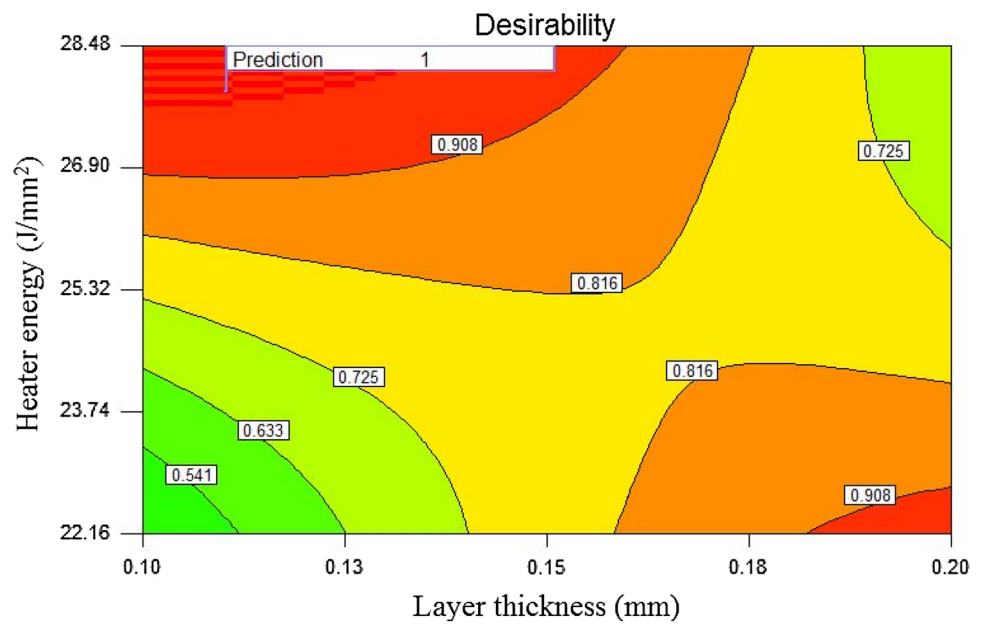


Table 5 Validation test results

| Process parameters | Optimum level | Predicted | Actual | Error % |
|------------------------------------|---------------|-----------|--------|---------|
| Layer thickness (mm) | 0.11 | 0.0208 | 0.0217 | 4.14 |
| Heater energy (J/mm ²) | 27.88 | | | |
| Heater feedrate (mm/s) | 3 | | | |
| Printer feedrate (mm/min) | 118.78 | | | |

3.5 Microstructure analysis

The micrographs presented in Fig. 9a–d illustrate the worn surfaces of HDPE specimens fabricated at diverse process parameters for sliding velocity of 1 m/s in evaluating dry sliding wear characteristics. The surface characteristics of part produced at optimal processing conditions reveals in Fig. 9a that indicates the accumulation and deformation

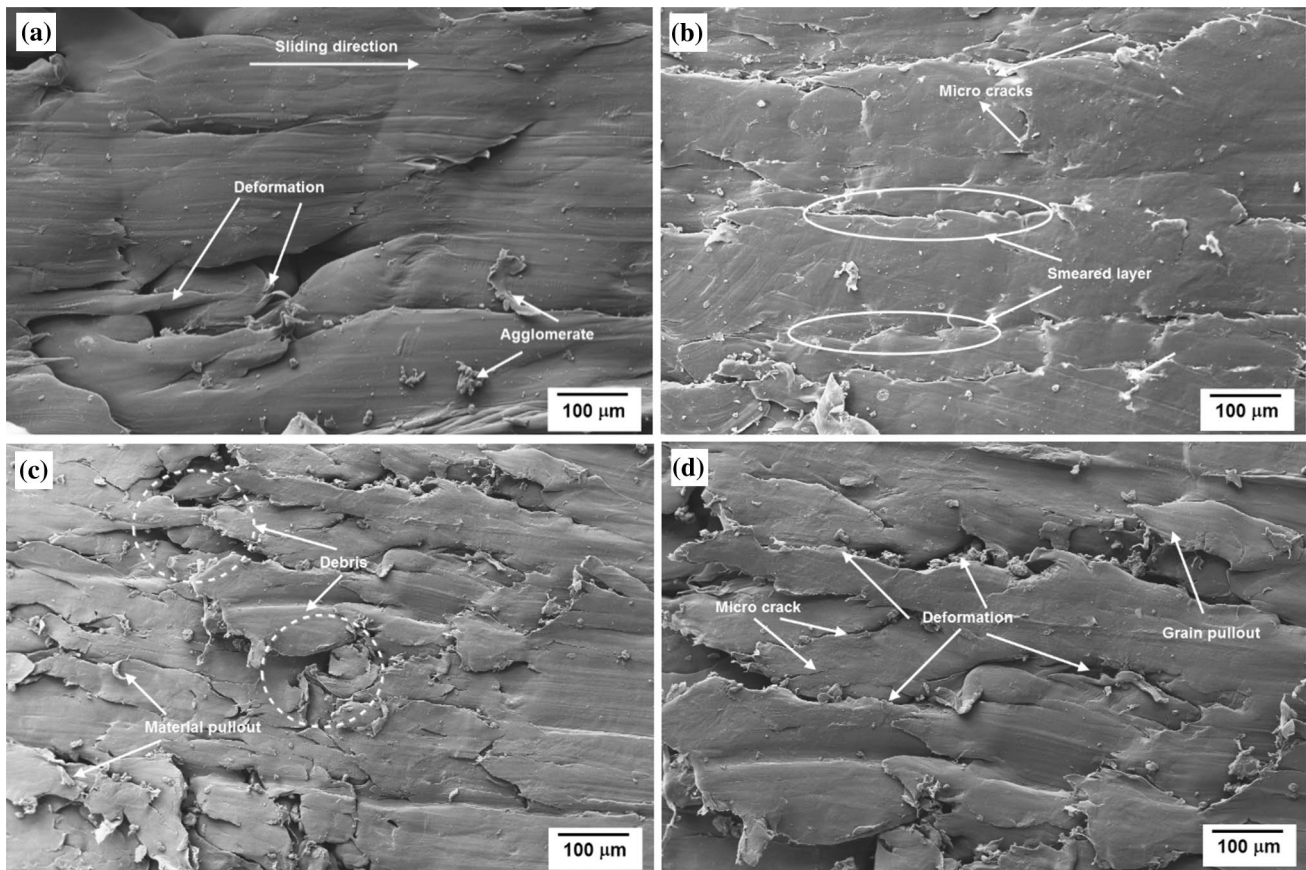


Fig. 9 SEM microphotographs of worn surfaces **a** $A=0.11$ mm, $B=27.88$ J/mm², $C=3$ mm/s, $D=118.78$ mm/min; **b** $A=0.15$ mm, $B=25.32$ J/mm², $C=3.25$ mm/s, $D=110$ mm/min; **c** $A=0.2$ mm,

$B=28.48$ J/mm², $C=3.5$ mm/s, $D=120$ mm/min; **d** $A=0.1$ mm, $B=22.16$ J/mm², $C=3$ mm/s, $D=100$ mm/min

of polymer particles are more at the counter side of sliding direction. The agglomeration of particles observed in the worn surface is scarcer because better fusion of powder particles produces dense structure with increased wear resistance.

The specimens built considering middle range of process parameters has experienced micro cracks and smeared layer in their worn surface as observed from Fig. 9b. It is due to insufficient heat delivery of sintered layers when layer thickness is increased. The augmented deformation, debris, polymer pull-out and major cracks are observed in the worn surfaces that fabricated at low and higher range of process parameters as shown in Fig. 9c, d. This could be caused because of improper sintering in the event of heating and cooling process, dislocation of layers and non-uniform temperature gradients. These SEM results confirm the wear trend observed in 3D surface plots (Fig. 6a–c) and indicate that the wear rate increased linearly with increasing layer thickness and decreasing heat energy.

3.6 Sensitivity analysis

Sensitivity analysis is performed to identify the qualitative and quantitative effectiveness of process parameters and rank them by their order of importance. It has remarkable importance in the model validation wherein attempts are made to compare the calculated output to the measured data [20]. Therefore, it plays a vital role in determining input process variables by exerting the most influence on the model outputs. The sensitivity of a design objective function with respect to a design variable is the partial derivative of that function with respect to its variables [21].

The purpose of the present study is to predict the tendency of wear rate with respect to various SIS process variables such as layer thickness, heater energy, heater feedrate and printer feedrate. The wear rate sensitivity equations are obtained by partially differentiating the Eq. 3 with respect to A , B , C and D . The following equations (Eqs. 4–7) represent the wear rate sensitivity for layer thickness (A), heater energy (B), heater feedrate (C) and printer feedrate (D), respectively:

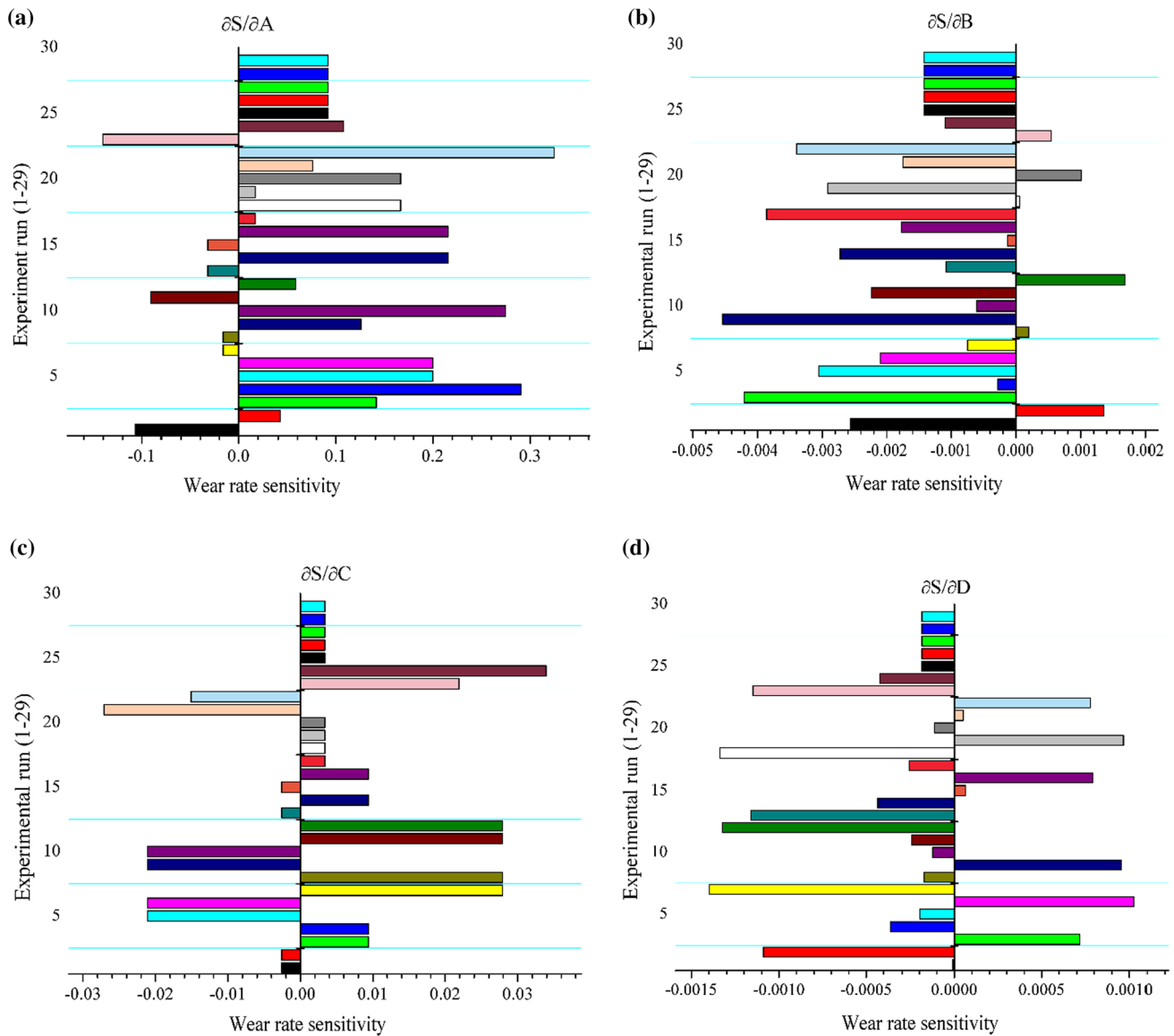


Fig. 10 Wear rate sensitivity of **a** layer thickness, **b** heater energy, **c** heater feedrate and **d** printer feedrate

$$\frac{\partial S}{\partial A} = 0.062358 + 0.039241 \times B - 0.0108 \times D + 1.492702 \times A, \quad (4)$$

$$\frac{\partial S}{\partial B} = -0.01955 + 0.039241 \times A + 0.001899 \times C + 0.000115 \times D - 0.00026 \times B, \quad (5)$$

$$\frac{\partial S}{\partial C} = -0.31418 + 0.001899 \times B + 0.00245 \times D, \quad (6)$$

$$\frac{\partial S}{\partial D} = -0.00284 - 0.0108 \times A + 0.000115 \times B + 0.00245 \times C - 6 \times 10^{-5} \times D. \quad (7)$$

If the wear rate sensitivity with respect to a certain process variable is positive, it implies an increment in the wear rate due to an increase in design variables [22]. The sensitivities of layer thickness (A), heater energy (B), heater feedrate (C) and printer feedrate (D) on wear rate are presented in Fig. 10a–d by solid bars with respect to various processing conditions as premeditated using BBD in Table 2. These results revealed that the layer thickness followed by heater feedrate is more sensitive on wear rate, whereas heater energy and printer feedrate have less sensitivity.

4 Conclusion

Prediction of wear rate using RSM based box-behnken design and finding optimal SIS process parameters through desirability approach is carried out. Response surface analysis yielded a better understanding on the influence of four SIS process parameters in evaluating wear rate of built specimens. The following observations have been made during the modeling and experimental studies:

- ANOVA results demonstrated that the layer thickness has significant effect on wear rate followed by heater energy. Moreover, strong interaction has been found between layer thickness and heater energy, heater feedrate and printer feedrate.
- Wear rate decreased with increase in heater energy, whereas it is increased with increase in layer thickness. Wear rate is not much influenced with increase in printer and heater feedrate.
- Minimal wear rate of $0.0208 \text{ mm}^3/\text{m}$ is attained at optimal SIS process parameters of 0.11 mm layer thickness, $27.88 \text{ J}/\text{mm}^2$ of heater energy, $3 \text{ mm}/\text{s}$ of heater feedrate, and $118.78 \text{ mm}/\text{min}$ of printer feedrate.
- The SEM micrographs of worn surfaces illustrate the wear debris, polymer pull-out and micro cracks due to uneven sintering and heat generation through continuous sliding motion.
- Sensitivity analysis revealed that the variations in layer thickness and heater feedrate are predominantly affected wear rate of fabricated SIS parts.
- Performed confirmation experiments agreed with an error of 4.14% between actual and predicted wear rate.
- The conformity of predicted results indicates that the proposed RSM-desirability approach can be effectively utilized in evaluating and determining optimal SIS process parameters.

Acknowledgements The authors would like to thank Science and Engineering Research Board (SERB), Project Ref. SB/EMEQ-179/2014, Department of Science and Technology, Government of India for the financial assistance.

References

1. Hilton PD, Jacobs PF (2000) Rapid tooling: technologies and industrial applications. Marcel Dekker, New York
2. Norazman F, Hopkinson N (2013) Effect of sintering parameters and flow agent on the mechanical properties of high speed sintered elastomer. Proceedings from the 24th SFF symposium, Austin, Texas, pp 368–379
3. Wang WL, Cheah CM, Fah JYH, Lu L (1996) Influence of process parameters on stereolithography part shrinkage. Mater Des 17(4):205–213
4. Mahapatra SS, Sood AK (2012) Bayesian regularization-based Levenberg–Marquardt neural model combined with BFOA for improving surface finish of FDM processed part. Int J Adv Manuf Technol 60:1223–1235
5. Gibson I, Shi D (1997) Material properties and fabrication parameters in selective laser sintering process. Rapid Prototyp J 3(4):129–136
6. Rouholamin D, Hopkinson N (2016) Understanding the efficacy of micro-CT to analyse high speed sintering parts. Rapid Prototyp J 22(1):152–161
7. Hopkinson N, Erasenthiren PE (2004) High speed sintering—early research into a new rapid manufacturing process. Proceedings from the 15th SFF symposium, Austin, Texas, pp 312–320
8. Khoshnevis B, Asiabanpour B, Mojdeh M, Palmer K (2003) SIS—a new SFF method based on powder sintering. Rapid Prototyp J 9(1):30–36
9. Asiabanpour B, Palmer K, Khoshnevis B (2004) An experimental study of surface quality and dimensional accuracy for selective inhibition of sintering. Rapid Prototyp J 10(3):181–192
10. Asiabanpour B, Khoshnevis B, Palmer K (2006) Advancements in the selective inhibition sintering process development. Virtual Phys Prototyp 1(1):43–52
11. Equbal A, Sood AK, Ohdar RK, Mahapatra SS (2010) Prediction and analysis of sliding wear performance of fused deposition modelling-processed ABS plastic parts. Proc Inst Mech Eng Parts J 224:1261–1271
12. Sood AK, Equbal A, Toppo V, Ohdar RK, Mahapatra SS (2012) An investigation on sliding wear of FDM built parts. CIRP J Manuf Sci Technol 5:48–54
13. Kumar S, Kruth JP (2008) Wear performance of SLS/SLM materials. Adv Eng Mater 10(8):750–753
14. Ramesh CS, Srinivas CK (2009) Friction and wear behaviour of laser-sintered iron-silicon carbide composites. J Mater Process Technol 209:5429–5436
15. Myers RH, Montgomery DC (1995) Response surface methodology: process and product optimization using designed experiments. Wiley, Inc., New York
16. Evans M (2003) Optimization of manufacturing processes: a response surface approach. Carlton House Terrace, London
17. Noordin MY, Vankatesh VV, Sharif S, Elting S, Abdullah A (2004) Application of response surface methodology in describing the performance of coated carbide tools when turning AISI 1045 steel. J Mater Process Technol 145:46–68
18. Derringer G, Suich R (1980) Simultaneous optimization of several response variables. J Qual Technol 12:214–219
19. Tamilarasan A, Rajamani D (2017) Multi-response optimization of Nd: YAG laser cutting parameters of Ti-6Al-4V superalloy sheet. J Mech Sci Technol 31(2):813–821
20. Kim IS, Son KJ, Yang YS, Yarangada PKDV. (2003) Sensitivity analysis for process parameters in GMA welding processes using a factorial design method. Int J Mach Tool Manuf 43(8):763–769
21. Lakshminarayanan AK, Balasubramanian V (2009) Comparison of RSM with ANN in predicting tensile strength of friction stir welded AA7039 aluminium alloy joints. T Nonferrous Metal Soc 19(1):9–18
22. Joardar H, Das NS, Sutradhar G, Singh S (2014) Application of response surface methodology for determining cutting force model in turning of LM6/SiCP metal matrix composite. Measurement 47:452–464